Droplet Growth in Binary Liquid Systems

RICHARD J. AYEN and J. W. WESTWATER

University of Illinois, Urbana, Illinois

Experimental measurements of the growth of liquid drops suspended in three different, supersaturated, binary liquid mixtures were made with cinephotomicrography. Diameters up to 5μ were reached in from 5 to 500 sec. Results for acetone drops and for isoamyl alcohol drops growing in glycerol solutions agree within 20 and 40% of the theoretical expression of Scriven with mass diffusivities estimated from the Wilke-Chang correlation. For glycerol drops in acetone, free convection was evident, and the experimental growth rates were lower than predicted by a factor of 5. Scriven's equation seems to be substantiated. Therefore, drop-growth measurements is a new method for obtaining liquid-liquid diffusivities, limited however to systems with negligible free convection.

Spherically symmetric phase change is found in many natural phenomena. Examples include the formation and growth of bubbles in liquids or of drops in vapors. In order to understand better these phenomena, it is desirable to determine the details of the phase change involved. A number of theoretical and experimental investigations have been undertaken to achieve this goal. The most complete theoretical analysis is that of Scriven (*1, 2*), who derived expressions for predicting growth rates of bubbles and drops for conditions of heat transfer controlling, mass transfer controlling, or a combination of these two conditions. His treatment includes both one-component and two-component systems. The Scriven predictions are the ones which will be used in this present paper.

Other theoretical analyses include those by Birkhoff, Margulies, and Horning (*3*); Epstein and Plesset (*4*); Doremus (*5*); and Bruijn (*6*) for conditions of mass transfer controlling. For heat transfer controlling, analyses have been given by Plesset and Zwick (*7*), Forster and Zuber (*8*), Birkhoff et al. (*3*), Bankoff and Mikesell (*9, 10*), Griffith (*11*), Forster (*12*), and others. The special case of cavity growth or collapse governed solely by mechanical forces was analyzed long before by Rayleigh (*13*).

Experimental measurements for bubble growth with heat transfer controlling have been made by Benjamin and Westwater (*14*); Strenge, Orell, and Westwater (*15*); Dergarabedian (*16, 17*); Van Wijk and Van Stralen (*18*); Staniszewski (*19*); Harrach (*20*); Chun (*21*); Ellion (*22*); Levenspiel (*23*); and others. Experimental data for mass transfer controlled growth, with negligible heat transfer, include bubble growth during electrolysis reported by Westerheide and Westwater (*24*) and Glas (*25*). Bubbles formed by dissolved gases in supersaturated solutions have been measured by Houghton, Ritchie, and Thomson (*26*); Doremus (*5*); Buehl and Westwater (*27*); and Manley (*28*).

The theoretical treatment of Scriven is of particular interest because it involves fewer assumptions than used by other workers. However, it does assume radial symmetry and a uniform initial supersaturation. Most existing data are for test conditions involving phase change on a wall, on bubbles which are rising, or with a nonuniform supersaturation. No data exist for the rate of liquid-liquid phase change with spherical symmetry. The purpose of this investigation was to supply this missing information by motion picture photography of growing liquid droplets in a bulk liquid phase, away from any walls or disturbances which could affect the concentration profiles, with controlled conditions with an accurately known driving force.

In brief, the method for achieving the phase change with a known driving force is indicated in Figure 1. This is the phase diagram for one of the binary liquid pairs. At time zero, a saturated liquid mixture, such as represented in Figure 1 by point A and temperature T_1 for Run 68, is cooled suddenly to a new temperature T_2. This supersaturated phase is essentially at T_2 for a distance large compared with droplet sizes. Nucleation occurs spontaneously, and the new phase grows as microscopic droplets suspended in the bulk phase. Motion picture photography through a microscope is used to record the growth of the droplets. A selection of the motion pictures is available upon request (*29*). A selection of photographic enlargements of single frames is available also (*30*).

THEORY

The concentration profiles near the liquid-liquid interface are indicated in Figure 2. Inside the drop, homogeneity is assumed to exist, and the solute concentration is given by $C_A = x_A\rho_A$. In the bulk phase the solute concentration is C_∞ at the start, but thereafter it is a function of distance and time. The overall driving force for mass transfer is the difference between C_∞ and the concentration in equilibrium with the drop C_s.

The density in each liquid phase is assumed to be constant. This is excellent for the drop phase. There is a slight variation in the bulk phase because of the concentration profile; a maximum variation of 1% was encountered in this study. The mass transfer is assumed to be by ordinary molecular diffusion only. This implies that no convection currents are present and that the drop size is so small that the rise or fall during a run is nil, as predicted by Stokes law. Additional assumptions are that the mass diffusivity is constant and that no chemical reactions occur. The heat of solution for the binary mixtures used was measured and found to be never greater than 0.9 cal./g. This is a very small value, so the systems were assumed to be isothermal.

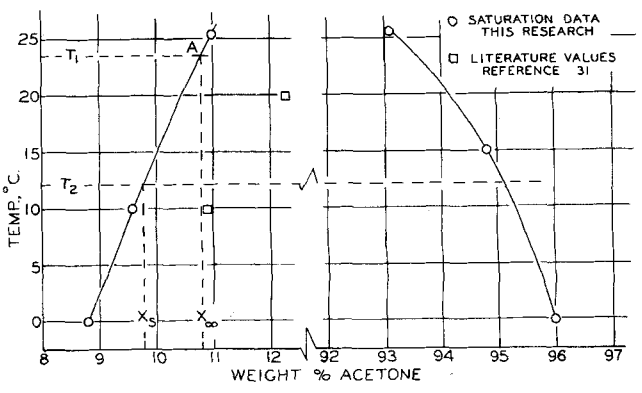

Fig. 1. Miscibility of acetone and glycerol. Binary pairs of these liquids were used for Systems 1 and 3.

R. J. Ayen is with the University of California, Berkeley, California.

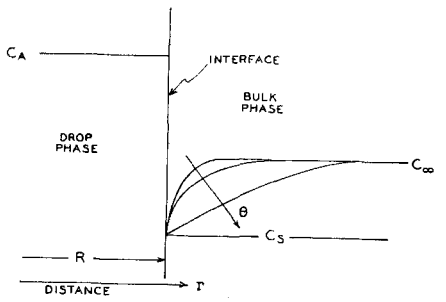

Fig. 2. Concentration profiles near the liquid-liquid interface.

For a growing liquid drop, the equation to be solved is Equation (1). Radial symmetry is implied:

$$\frac{\delta C}{\delta \theta} + u\frac{\delta C}{\delta r} = D\left(\frac{\delta^2 C}{\delta r^2} + \frac{2}{r}\frac{\delta C}{\delta r}\right) \qquad (1)$$

The center of the drop is the center of the coordinate system. The continuity equation may be combined with an overall mass balance to yield the radial velocity of the bulk liquid surrounding the droplet u as shown in Equation (2):

$$ur^2 = \epsilon R^2 \frac{dR}{d\theta} \qquad (2)$$

A necessary boundary condition is given by a solute balance at the interface, Equation (3):

$$x_A\rho_A\frac{dR}{d\theta} = C_s(1-\epsilon)\frac{dR}{d\theta} + D\frac{\delta C}{\delta r}\bigg|_{r=R} \qquad (3)$$

The remaining boundary conditions are that $C = C_\infty$ at all positions at time zero, $C = C_s$ in the bulk liquid at $r = R$ at all subsequent times, and $C = C_\infty$ at $r = \infty$ at all times.

The form of the radius vs. time function must be assumed. Scriven used Equation (4):

$$R = 2\beta\sqrt{D\theta} \qquad (4)$$

Scriven's derivation (*1*) results in the final expression, Equation (5):

$$\Phi = 2\beta^3 \exp(\beta^2 + 2\epsilon\beta^2)\int_\beta^x x^{-2}\exp(-x^2 - 2\epsilon\beta^3 x^{-1})\,dx \qquad (5)$$

where

$$\Phi = \frac{\rho_B(C_\infty - C_s)}{\rho_A(x_A\rho_B - C_s)} \qquad (6)$$

Equation (5) was solved by Scriven using numerical techniques. The result is a tabulation of values of the growth constant β for various values of ϵ and Φ. These values were used in the present research. A graph of the theoretical relationship of β vs. Φ for ϵ values ranging from -0.5 to $+0.33$ is the solid line in Figure 7.

EXPERIMENTAL

Three systems were studied, chosen so as to give a good variation in physical properties.

System 1., Droplets of acetone saturated with glycerol were grown in glycerol supersaturated with acetone.

System 2. Droplets of isoamyl alcohol saturated with glycerol were grown in glycerol supersaturated with isoamyl alcohol.

System 3. Droplets of glycerol saturated with acetone were grown in acetone supersaturated with glycerol.

For these systems, the viscosity of the bulk phase ranged from about 0.4 to about 1,000 centipoise. The solute diffusivity ranged from about 10^{-5} to about 10^{-6} sq.cm./sec. The ratio of drop density to the bulk phase density ranged from about 0.7 to about 1.5. The overall concentration driving force $C_\infty - C_s$ was varied for each system by a factor of as great as 7 to 1.

The chemicals met the American Chemical Society specifications for reagent grade. Glycerol, isoamyl alcohol, and acetone were used. The saturated binary liquid mixtures needed to start each run were prepared and stored in a constant temperature room set for 25°C. Equal volumes of the two components were mixed thoroughly in closed flasks and allowed to equilibrate and separate. Both layers remained cloudy for several days; the solutions were not used until they became clear.

To make a run, a saturated binary mixture was placed in the test cell sketched in Figure 3. This was a rectangular chamber about ¾ in. high, ½ in. wide, and ⅛ in. deep. The bottom and two ends were of one-piece construction, machined from Teflon. The back piece was a microscope slide glass, and the front piece was a microscope cover glass. These were sealed to the Teflon with an epoxy cement. The top cover was of silicone rubber. The cell held about 0.77 cc. of fluid and was easily fastened to the stage of a horizontal microscope.

A hollow stainless steel tube of 0.080-in. O.D. passed through the cell parallel to the glass windows. When desired, cold water was passed through the tube, and this brought about the sudden temperature change which caused phase change to occur. The coolant tube was located very close to the window near the microscope objective. Thus, the coolant tube and the adjacent liquid could be viewed at magnifications up to 500X.

Figure 4 indicates the arrangement of the coolant system. The bleed line permitted the removal of air bubbles and permitted precooling of the lines before the start of a run. The coolant temperature was determined as indicated in Figure 4 with a thermocouple located within about 1 in. of the test cell.

The original temperature of the liquid in the test cell was the temperature of the constant temperature room in which all tests were conducted. On most days this was 25°C. As soon as the coolant flow was started, the saturated liquid in the cell cooled very rapidly. The microscope was aimed so that the top edge of the coolant tube was near the bottom of the motion picture frames when films were taken through the microscope. At a magnification of 70X, the field of view was all within 0.004 in. of the cold tube. Experimental techniques for measuring the temperature profile within this tiny region are not available. Calculations show that all this region would approach to within 95% of the possible temperature change within 13 sec. This is in strong contrast to the 55 hr. required to approach within 95% of concentration equilibrium by mass diffusion for acetone in glycerol. The rate of heat conduction is enormous compared with the rate of mass diffusion; therefore, the temperature change may be treated as being in one step. However, in the interest of maximum accuracy, the unsteady temperature behavior was taken into account for all measurements at short times. The necessary correction never exceeded 5%.

The microscope with the test cell on its stage was mounted on a horizontal optical bench. Illumination was provided by a ribbon-filament lamp operating at 17 amp. and 6 v. A condenser, iris, filter, and a water-filled cooling cell were traversed by the light beam before it passed through the test cell. From the test cell the light passed through a microscope having an 8 mm., 0.50 N.A. objective and an 8X eyepiece. A 16-mm. motion picture camera viewed through the microscope. Distances were adjusted so that the magnification of the image on

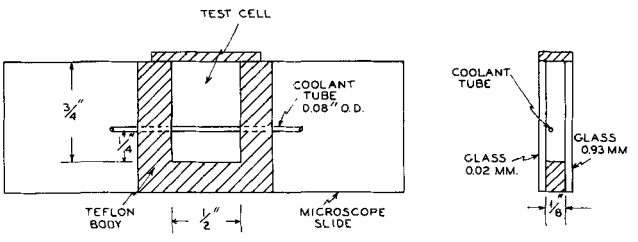

Fig. 3. Details of test cell. Rapid flow of cold water through the coolant tube caused a virtually one-step temperature change in the saturated mixture in the test cell.

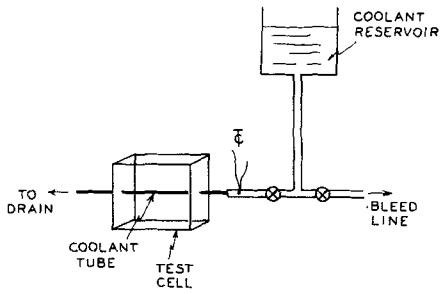

Fig. 4. Arrangement of coolant flow system. Not to scale.

the movie film usually was about 70X. The exact calibration was made with a micrometer slide.

Two movie cameras were used, a reflex model for 100-ft. film reels, and a model 05 camera for 400-ft. reels. Framing rates were 14.10 frames/sec. for System 1, 24.00 for System 2, and 15.42 for System 3. No lenses were used on either camera; all magnification was due to the microscope lenses.

An electric reversing motor was connected to the fine focus adjustment on the microscope. This operated during a run so as to move the microscope barrel alternately forward and backward with a period adjusted between 2 and 6 sec. For the early runs this reciprocating action was done manually. The motion caused the plane of focus of the microscope to sweep through a volume measuring about 0.007 in. front to back. This procedure had an important advantage. It meant that all the drops in a known volume of liquid could be brought into focus, each one periodically, during a run. A good measurement of the diameter could be obtained each time a particular drop came into focus. The corresponding time was known from the frame number of the movie film.

For each run, time zero was taken as the instant the coolant first flowed through the coolant tube. The camera was started at this instant. The duration of a run was between 1 and 12 min. The resulting motion picture films were measured on a motion analyzer. This instrument permitted measurements to within 0.0001 in. on the film (about 1.4×10^{-6} in. in the test cell); however, the actual drop boundary was not distinct enough to utilize this much accuracy. Drop diameter vs. time, the distance from a drop to the coolant tube, and the distance from a drop to its nearest neighbor were read from the films.

The experimental work included measurement of the densities of all phases used, viscosities of the bulk phases involved, and the miscibility data for each system. Details of this work are available (*30*). The measured miscibilities for one system are given here in Figure 1. The new miscibility values are somewhat different from prior values. The prior measurements were made many years ago (*31*), and it may be possible that the purities of the test liquids were different. In any case, the values used for the present work are the new ones.

RESULTS

Conditions for a typical test, Run 68, are indicated in Figure 1. The stepwise temperature change was from 23.7° to 12.3°C. which established an overall driving force for mass transfer of $x_\infty - x_s = 0.1086 - 0.0990$, in units of weight fraction of acetone. The droplet composition read from Figure 1 is 0.951 wt. fraction acetone. From a knowledge of the phase densities, one gets $\epsilon = 0.329$, and using Equation (6) one gets $\Phi = 0.0168$. The solid line in Figure 7 shows that the predicted value of the growth coefficient is $\beta = 0.11$.

For System 1, the stepwise temperature change was varied from 5° to 15°C.; for System 2 it varied from 2° to 7°C., and for System 3 it varied from 1° to 7°C. The range of predicted values of β was 0.0047 to 0.14. Experimentally, the time for a drop to achieve a diameter of 5μ varied from about 5 to 500 sec.

Experimental values of the growth coefficient β were determined for 119 drops. For each drop this was done by taking the slope of a graph of (diameter) squared vs. time. One typical drop for each of the three systems is illustrated in Figures 5 and 6. The slope of the graph is $16\ \beta^2 D$, and β is fixed from a knowledge of the diffusivity D.

Unfortunately, experimental values for the diffusivities are not available. Therefore, the Wilke-Chang empirical correlation (*32*) was used to estimate the values of D. The correlation requires a knowledge of liquid viscosity. They were measured for this work (*30*). The correlation requires the choice of an association parameter. This value is unknown for the systems used here. An estimated value of 1.5 was selected as being reasonable and within the expected limits of 1.0 and 2.6. The value of D is a function of the square root of this parameter. At 20°C. the estimated values used for D were 6.1×10^{-8} sq.cm./sec. for System 1, 1.6×10^{-8} for System 2, and 3.53×10^{-5} for System 3. It must be borne in mind that these are of unknown accuracy. Fortunately, the resulting uncertainty in β is but the square root of the error in D, because the number directly computed from the drop-growth data is the product $\beta^2 D$. This means that the association parameter enters only to the one-fourth power, as far as its effect on β is concerned.

The results of all determinations of the growth coefficient β are given in Figure 7. Every symbol on this graph is representative of the complete growth curve of one drop. If one assumes that the diffusivities used are qualitatively correct, then the growth data for Systems 1 and 2 substantiate the final Scriven analysis in an excellent manner. System 3 gives less good agreement. The fact that the (diameter) squared vs. time growth curves, such as shown in Figures 5 and 6, are straight lines substantiates Equation (4), the general equation assumed by Scriven.

If the assumed diffusivities are considered as correct quantitatively, then the actual growth coefficients β for System 1 are low by about 20% on the average, and they are low by about 40% for System 2. System 3 gives β values low by a factor of about 5. The present writers interpret this agreement for Systems 1 and 2 to mean that Scriven's analysis should be interpreted as correct and that the diffusivities used are not quite right. The disagreement for System 3 is too great to be accountable by its diffusivity. Possibly the data for System 3 can logically be explained as a result of convection, as follows.

For Systems 1 and 2 the bulk phase was mostly glycerine. The viscosity was great, and free convection was minor. For occasional runs, droplet translation was evident, and in these cases the entire run was discarded. For the runs used, the translation was near zero.

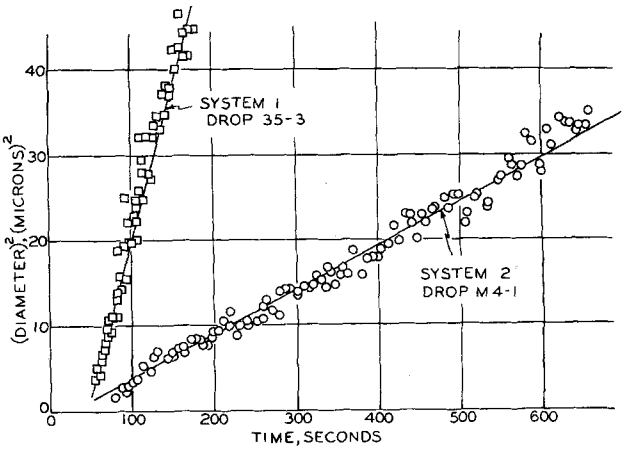

Fig. 5. Typical drop growth data. For the System 1 droplet, the stepwise temperature change was from 25.8° to 20.6°C. For the System 2 droplet, the change was from 24.1° to 17.5°C.

However, for System 3 the bulk phase was mostly acetone, and some translation was evident for all drops. A drop was visible for about five motion picture frames before moving out of the field of view. The rate of fall was in the order of 20 μ/sec. which is roughly as predicted from Stokes's law. For falling drops the Scriven analysis is not applicable.

For drops falling toward the coolant tube, as occurred for System 3, one might expect the growth to be greater than predicted for stationary drops. This was not observed. Because of the relatively high diffusivity for this system, the concentration profile surrounding each drop extended far enough to overlap with the concentration profiles for neighboring drops. Besides this, it is possible that free convection was causing the bulk liquid to move in such a way as to surround the drops with a lean mixture, or the convection altered the temperature profile enough that the concentration driving force was less than expected. Of course, some error in the estimated diffusivity is possible also. At present the correct explanation is unknown.

For all systems the population of growing drops was a function of the driving force. For large values of ΔC the drops were so numerous that they exerted an influence on one another as their sizes became comparable to the clearance between them. In such cases the growth curves, (diameter) squared vs. time, were straight lines at small times but then curved down at higher times. The slopes at small times were used to get β for these drops. The population of nucleation sites increased with the age (elapsed time after mixing) of the solutions, but this did not affect the growth constant. Presumably the nucleation sites were invisible impurities, too small to be detected under the microscope. No impurities were put in the systems, and clean laboratory techniques were observed.

DIFFUSIVITY MEASUREMENT BY DROP GROWTH

The rate of solution of gas bubbles has been used by Houghton et al. (*26*) to measure gas-liquid diffusivities. Their published values must be somewhat in error, because their bubbles were on a wall and their theoretical equation had some approximations. However, for the liquid-liquid drop growth scheme described in the present paper, the drops are spheres, they are remote (relative to their sizes) from a wall, and the Scriven analysis is more precise.

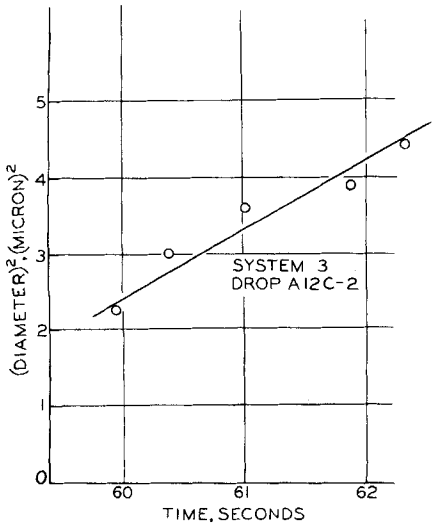

Fig. 6. Typical drop growth data for System 3. The stepwise temperature change was from 25.50° to 23.26°C.

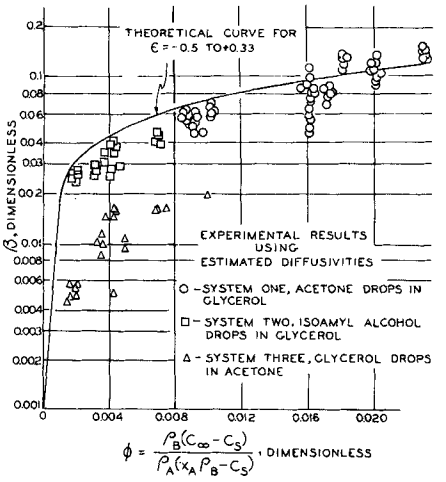

Fig. 7. Comaprison of theoretical and experimental drop-growth coefficients.

If one assumes the Scriven analysis is exact, the drop-growth scheme definitely can be used to measure liquid-liquid diffusivities. Required information includes miscibility data over a range of temperatures, the growth rate of a drop growing in a supersaturated solution (or the rate of solution in an unsaturated solution), and densities of both phases. Advantages of the method are that the actual amount of solute transferred need not be measured, actual concentration profiles need not be measured, and the duration of a test run is short. One disadvantage is that the method is not valid if free convection is present.

The drop-growth method predicts $D = 4 \times 10^{-8}$ sq. cm./sec. for 10 wt. % acetone in glycerol at 17°C. and 1×10^{-8} sq.cm./sec. for 4 wt. % isoamyl alcohol in glycerol at 20°C. When independent measurements of these diffusivities become available, the usefulness of the suggested method may be certified.

ACKNOWLEDGMENT

Graduate fellowships were provided by the Monsanto Company and the University of Illinois. Additional financial assistance was furnished by the National Science Foundation.

NOTATION

(Dimensions in the $ML\theta T$ system)

- C = concentration of solute, M/L^3
- D = mass diffusivity, L^2/θ
- r = radial distance from center of drop out into the bulk phase, L
- R = drop radius, L
- u = radial velocity of bulk phase at position r and time θ, L/θ
- x = mass fraction of solute in liquid, dimensionless
- β = growth coefficient defined by Equation (4), dimensionless
- ϵ = density factor = $1 - (\rho_A/\rho_B)$, dimensionless
- ρ = density, M/L^3
- Φ = dimensionless driving force, defined by Equation (6)
- θ = time, θ

Subscripts

- A = droplet phase
- B = bulk phase
- s = value at saturation
- ∞ = value at large r

LITERATURE CITED

1. Scriven, L. E., *Chem. Eng. Sci.*, **10**, 1 (1959).
2. *Ibid.*, **17**, 55 (1962).
3. Birkhoff, Garrett, R. S. Margulies, and W. A. Horning, *Physics of Fluids*, **1**, 201 (1958).
4. Epstein, P. S., and M. S. Plesset, *J. Chem. Phys.*, **18**, 1505 (1950).
5. Doremus, R. H., *J. Am. Ceram. Soc.*, **43**, 655 (1960).
6. Bruijn, P. J., *Physica*, **26**, 326 (1960).
7. Plesset, M. S., and S. A. Zwick, *J. Appl. Phys.*, **25**, 493 (1954).
8. Forster, H. K., and Novak Zuber, *ibid.*, p. 474.
9. Bankoff, S. G., and R. D. Mikesell, *Chem. Eng. Progr. Symposium Ser. No. 29*, **55**, 95 (1959).
10. ————, *paper 58-A-105*, Am. Soc. Mech. Engrs.
11. Griffith, Peter, *Trans. Am. Soc. Mech. Engrs.*, **80**, 721 (1958).
12. Forster, K. E., *Physics of Fluids*, **4**, 448 (1961).
13. Rayleigh, Lord, *Phil. Mag.*, **34**, 94 (1917).
14. Benjamin, J. E., and J. W. Westwater, "International Developments in Heat Transfer," p. 212. The American Society of Mechanical Engineers, New York, New York (1963).
15. Strenge, P. H., Aluf Orell, and J. W. Westwater, *A.I.Ch.E. Journal*, **7**, 578 (1961).
16. Dergarabedian, Paul, *J. Appl. Mechanics*, **20**, 537 (1953).
17. ———, *J. Fluid Mech.*, **9**, part 1, p. 39 (1960).
18. Van Wijk, W. R., and S. J. D. Van Stralen, *Physica*, **28**, 150 (1962).
19. Staniszewski, E. E., *Tech. Report No. 16*, Division of Sponsored Research, Massachusetts Institute of Technology, Cambridge, Massachusetts (1959).
20. Harrach, W. G., Ph.D. thesis, Lehigh University, Bethlehem, Pennsylvania (1960).
21. Chun, K. S., Ph.D. thesis, Illinois Institute of Technology, Chicago, Illinois (1956).
22. Ellion, M. E., *Jet Propulsion Lab., Memo 20-88*, California Institute of Technology, Pasadena, California (1954).
23. Levenspiel, Octave, *Ind. Eng. Chem.*, **51**, 787 (1959).
24. Westerheide, D. E., and J. W. Westwater, *A.I.Ch.E. Journal*, **7**, 357 (1961).
25. Glas, J. P., Ph.D. thesis, University of Illinois, Urbana, Illinois (1964).
26. Houghton, G., P. D. Ritchie, and J. A. Thomson, *Chem. Eng. Sci.*, **17**, 221 (1962).
27. Buehl, W. M., and J. W. Westwater, in preparation.
28. Manley, D. M. J. P., *Brit. J. Appl. Phys.*, **11**, 38 (1960).
29. Westwater, J. W., and R. J. Ayen, Motion Picture, "Growth of Droplets in a Binary Liquid System," University of Illinois, Urbana, Illinois (1964).
30. Ayen, R. J., Ph.D. thesis, University of Illinois, Urbana, Illinois (1964).
31. McEwen, B. C., *J. Chem. Soc. (London)*, **123**, 2279 (1923).
32. Wilke, C. R., and Pin Chang, *A.I.Ch.E. Journal*, **1**, 264 (1955).

Manuscript received February 10, 1964; revision received May 11, 1964; paper accepted May 12, 1964.

Binary Liquid-Phase Adsorption Equilibria

JOHN F. WALTER and EDWARD B. STUART

University of Pittsburgh, Pittsburgh, Pennsylvania

At present a number of empirical models exist describing binary liquid-phase adsorption equilibria. Vermeulen (*1*) reviewed a number of empirical liquid-phase correlations. Some of these correlations are analogies of common gas-phase adsorption isotherm equations, such as the Freundlich, Langmuir, and B.E.T. isotherm equations. Another correlating equation was offered by Stuart and Coull (*2*). Perhaps the most commonly used correlating equation is known as the Gibbs-Duhem isothermal-isobaric equation (*3, 4*):

$$\frac{y}{1-y} = \alpha \frac{x}{1-x} \qquad (1)$$

The relative adsorptivity is determined empirically and is sometimes assumed to be constant. Although most of these correlating equations have semitheoretical bases, they are all used empirically and for the most part do not provide insight into effects of variation in molecular properties, temperature, pore diameter, and adsorbent properties.

With the discovery by London of dispersion forces, the forces causing physical adsorption are reasonably well understood. These forces are discussed and summarized by de Boer (*5*). As de Boer shows and as will be discussed again in the following, the attractive potential energy for an adsorbate molecule to an adsorbent is proportional to the inverse cube of the separation distance. In the case of porous adsorbents, these forces are also dependent upon the pore structure, such as pore diameter or curvature, and surface composition. It is often stated that physical adsorption should be independent of the adsorbent used; this is not strictly true. Variations in the ionization poten-

J. F. Walter is presently with the Westinghouse Electric Corporation, Bettis Atomic Power Laboratory, Pittsburgh, Pennsylvania.